

# Enhanced nitrate reduction and current generation by *Bacillus* sp. in the presence of iron oxides

Wei Zhang · Xiaomin Li · Tongxu Liu · Fangbai Li

Received: 20 October 2011 / Accepted: 12 December 2011 / Published online: 11 January 2012  
© Springer-Verlag 2011

## Abstract

**Purpose** Fe(III) has been reported as a strictly competitive electron acceptor with respect to other substrate reductions by dissimilatory Fe(III)-reducing bacteria (DIRB). However, the effect of Fe(III) oxides on the substrate reduction by other microorganisms remain unknown. The aims of this study were to investigate the effects of iron oxides on the nitrate reduction and current generation by *Bacillus* sp., in which the nitrate and carbon anodes served as soluble and insoluble electron acceptors, respectively.

**Materials and methods** Microbial nitrate reduction by *Bacillus* sp. were conducted in batch cultures in the absence or presence of four chemically synthesized iron(III) oxyhydroxides [i.e.,  $\alpha$ -FeOOH,  $\gamma$ -FeOOH,  $\alpha$ -Fe<sub>2</sub>O<sub>3</sub>, and  $\gamma$ -Fe<sub>2</sub>O<sub>3</sub>]. Anaerobic techniques were used throughout all the

experiments. NO<sub>3</sub><sup>-</sup>/NO<sub>2</sub><sup>-</sup> was determined by ion chromatography, and NH<sub>4</sub><sup>+</sup> was measured by spectrophotometry at 420 nm after a color reaction with Nessler's reagent. For total Fe(II) determination, samples were extracted using 0.5 M HCl and tested by spectrophotometry at 510 nm, and Fe(II) analyses in NO<sub>3</sub><sup>-</sup> containing samples were performed using a sequential extraction technique. Current generation was tested using a bioelectrochemical reactor that consisted of two identical chambers separated by a cation exchange membrane.

**Results and discussion** The results showed that four iron oxides markedly enhanced the nitrate reduction and current generation by *Bacillus* sp. Nitrate reduction by the Fe(II) on the oxide surface was proven to take place, but with lower reduction rate than the direct microbial nitrate reduction by *Bacillus* sp. Al<sub>2</sub>O<sub>3</sub> and TiO<sub>2</sub>, as control without Fe(II) formation, also enhanced the nitrate reduction and current generation. It was proposed that the electron may be transferred from *Bacillus* sp. to conduction band of iron oxides to the nitrate or anode, according to their redox potential ranking as outer membrane enzyme of microorganisms < conduction band of iron oxides < electron acceptors.

**Conclusions** This study demonstrated that the presence of iron oxides can obviously enhance both the nitrate reduction and current generation by *Bacillus* sp., which was in contrast to the previous report with respect to the inhibition effect of Fe(III) on substrate reduction by DIRB. With respect to the semiconductive properties of iron oxides, their roles during the nitrate reduction and current generation were speculated as a conduction band of iron oxides mediating the electron transfer from *Bacillus* sp. to the nitrate and anode.

**Keywords** Current generation · *Bacillus* sp. · Iron oxides · Iron reduction · Nitrate reduction · Semiconductors

---

Responsible editor: Huijun Zhao

W. Zhang  
Guangzhou Institute of Geochemistry,  
Chinese Academy of Sciences,  
Guangzhou 510640, People's Republic China

T. Liu (✉) · F. Li (✉)  
Guangdong Key Laboratory of Agricultural Environment  
Pollution Integrated Control, Guangdong Institute  
of Eco-Environmental and Soil Sciences,  
510650 Guangzhou, People's Republic of China  
e-mail: txliu@soil.gd.cn  
e-mail: cefbli@soil.gd.cn

X. Li  
College of Natural Resources and Environment, South China  
Agricultural University,  
Guangzhou 510642, People's Republic of China

W. Zhang  
Graduate School of the Chinese Academy of Sciences,  
Beijing 100039, People's Republic of China

## 1 Introduction

Iron is common and abundant transition metal element on earth, especially in the iron-rich environments, e.g., red soil in South China. The iron reduction has a profound influence on the transformation of other elements and contaminants, e.g., carbon, nitrogen, and metals (Borch et al. 2010; Lovley et al. 2004; Li et al. 2010). The insoluble Fe(III) minerals are the most abundant forms of iron at circumneutral pH environments. In anoxic conditions, the Fe(III) reduction to Fe(II) was dominated by dissimilatory iron(III)-reducing bacteria (DIRB), which can use Fe(III) oxides as extracellular electron acceptor for their growth coupled with organic matter oxidation, which results in decomposition of organic matters to lower molecular weight organic acids and CO<sub>2</sub> (Lovley et al. 2004). However, many other electron acceptors (or substrates), e.g., nitrate, sulfate, humic substances, and manganese minerals, coexist in the natural environment, which may lead to a complicated interaction (e.g., inhibition and enhancement) between their reductions (Borch et al. 2010; Nevin et al. 2003).

Thus far, most of the reports used DIRB as the target microorganisms to study the interactions of various substrate reductions, and Fe(III) has been reported as a strictly competitive electron acceptor with respect to other substrate reductions by many DIRB, e.g., *Geobacter*, *Shewanella*, and *Desulfotomaculum* species (Lovley et al. 2004; Behrends and Van Cappellen 2005; Weber et al. 2006). However, few research was to investigate the effect of Fe(III) oxide on the substrate reduction of the other microorganisms. In the iron-bearing environments, many fermentative microorganisms were reported with weak ability of Fe(III) reduction, but the fermentative microorganisms are considered to be responsible for the production of fermentation products, which serve as electron donors for the iron reduction by the DIRB. However, other coexisting substrates, e.g., nitrate and humic substances, can be reduced by many fermentative microorganisms, e.g., *Escherichia* and *Klebsiella* species (Gonzalez et al. 2006; Li et al. 2009; Moreno-Vivián et al. 1999; Zhang et al. 2009), and the abundance of fermentative microorganisms is usually 1 or 2 orders of magnitude higher than the DIRB (Reiche et al. 2008). *Bacillus* sp., as a representative fermentative bacteria, has been reported as capable of Fe(III) reduction under anaerobic conditions (Kanso et al. 2002; Boone et al. 1995; Cheng and Li 2009; Pollock et al. 2007). But, the effect of iron oxides on the reduction of other coexisting substrates by *Bacillus* sp. remains unclear.

Among the reduction of different coexisting substrates, nitrate reduction plays a key role in the nitrogen cycle and has important agricultural, environmental, and public health implications (Moreno-Vivián et al. 1999; Shen et al. 2010; Xing et al. 2010). It was dominantly attributed to the direct

enzyme catalysis of microorganisms as well (Cabello et al. 2004; Gonzalez et al. 2006). Many *Bacillus* sp. were able to use nitrate and its reduction product, nitrite, as nitrogen sources for biosynthesis (assimilatory nitrate reduction), or as electron acceptors for anaerobic respiration (dissimilatory nitrate reduction; Espinosa-de-los-Monteros and Martinez 2001; Dou et al. 2010; Rajakumar et al. 2008). Natural nitrate reduction is usually coupled with iron cycles in the iron-bearing subsoil or sediment (Cooper et al. 2003; Coby and Picardal 2005; Wang et al. 2009). When goethite served as solid-phase Fe(III) source, the rates of microbial nitrate and nitrite reductions by *Shewanella putrefaciens* 200 were decreased significantly (Cooper et al. 2003). Moreover, the adsorbed Fe(II) generated from microbial reduction of iron minerals can reduce nitrate slowly in anaerobic sedimentary environments (Ottley et al. 1997). However, few studies have considered the effects of insoluble iron minerals on nitrate reduction by *Bacillus* sp.

Recently, anodes have been used as an alternative insoluble electron acceptor for microbial electricity collection in microbial fuel cells (MFCs; Nimje et al. 2009; Choi et al. 2001). The current generation by many microorganisms was mainly via outer membrane proteins, self-secreting chelators, and electron shuttles, or possible nanowires (Reguera et al. 2005; Hernandez and Newman 2001). The presence of soluble mediators, e.g., humic acid, has been proved to accelerate the electron transfer from microorganisms to anodes (Thygesen et al. 2009), and the iron oxides were also reported to facilitate long-distance electron transport through constructing electrically conductive networks with iron nanoparticles and DIRB (Nakamura et al. 2009a). *Bacillus* sp. has been reported to be an electroactive bacterium for current generation (Nimje et al. 2009; Choi et al. 2001). However, no study considers the effect of iron oxides on the current generation by *Bacillus* sp. in the bioelectrochemical system.

The objectives of this work are as follows (1) to investigate the effect of iron oxides on the reduction of the soluble substrates (nitrate/nitrite) by *Bacillus* sp., (2) to study the effect of iron oxide on the reduction of an insoluble substrate (anode) for current generation by *Bacillus* sp., and (3) to propose a possible interaction mechanism between the *Bacillus* sp., iron oxides, and electron acceptors.

## 2 Materials and methods

### 2.1 Materials

A fermentative bacterium, *Bacillus* sp., was isolated in our laboratory, which can reduce nitrate to nitrite under anaerobic condition. As described previously (Li et al. 2009), goethite ( $\alpha$ -FeOOH) was synthesized by dissolving Fe(NO<sub>3</sub>)<sub>3</sub>·9H<sub>2</sub>O in potassium hydroxide; lepidocrocite ( $\gamma$ -

FeOOH) was formed by mixing  $\text{FeCl}_2 \cdot 4\text{H}_2\text{O}$ ,  $(\text{CH}_2)_6 \text{N}_4$ , and  $\text{NaNO}_2$  in deionized water; hematite ( $\alpha\text{-Fe}_2\text{O}_3$ ) was prepared by sintering  $\gamma\text{-FeOOH}$  powder at  $420^\circ\text{C}$  for 2 h at a temperature increase rate of  $2^\circ\text{C min}^{-1}$ . Maghemite ( $\gamma\text{-Fe}_2\text{O}_3$ ) was synthesized using  $\text{FeCl}_2$ ,  $(\text{CH}_2)_6 \text{N}_4$ , and  $\text{NaNO}_3$  (Wang et al. 2008).  $\text{TiO}_2$  (Degussa P-25, with 80% anatase and 20% rutile) and  $\text{Al}_2\text{O}_3$  (Alu-C, 13 nm) were purchased from Degussa AG Company, Germany. All the iron and non-iron oxides were ground to pass through a 100-mesh sieve before use.  $\text{NaNO}_3$  ( $\geq 99.0\%$ ),  $\text{NaNO}_2$  (99.5%), and Nessler's reagent were obtained from Sigma-Aldrich and used without further purification. Other chemicals with analytical grade were from the Guangzhou Chemical Reagent Factory, China.

## 2.2 Nitrate/nitrite reduction experiments

Cells of *Bacillus* sp. were grown in a nutrient broth under an aerobic condition on a rotary shaker at 180 rpm at  $30^\circ\text{C}$  and harvested by centrifugation at  $6,900 \times g$  for 10 min at  $4^\circ\text{C}$  when it approached the exponential phase. The pellets were washed three times, after which they were resuspended in sterile deionized water. To avoid the interference of other inorganic anions in detection, the anaerobic  $\text{NaHCO}_3$ -buffered (30 mM, pH 6.8, with  $\text{N}_2/\text{CO}_2=80:20$  atm) medium only consisted of 7.0 mM  $\text{NaNO}_3$  or  $\text{NaNO}_2$  as an electron acceptor and 5 mM glucose as an electron donor, and harvested cells of *Bacillus* sp. with a final concentration of ca.  $10^7$  cells  $\text{mL}^{-1}$  were added. Several batch experiments for  $\text{NO}_3^-$  or  $\text{NO}_2^-$  reduction were conducted under different conditions: (1) *Bacillus* sp.; (2) *Bacillus* sp. + iron oxides (IOs, including  $\alpha\text{-FeOOH}$ ,  $\gamma\text{-FeOOH}$ ,  $\alpha\text{-Fe}_2\text{O}_3$ , and  $\gamma\text{-Fe}_2\text{O}_3$ ,  $4.5 \text{ g L}^{-1}$ ) (3) *Bacillus* sp. + non-Fe oxides ( $\text{TiO}_2$  and  $\text{Al}_2\text{O}_3$ ,  $4.5 \text{ g L}^{-1}$ ); (4) abiotic controls:  $\text{Fe}^{2+}$  (0.7 mM);  $\alpha\text{-FeOOH}$  ( $4.5 \text{ g L}^{-1}$ );  $\text{Fe}^{2+}$  (0.7 mM) +  $\alpha\text{-FeOOH}$  ( $4.5 \text{ g L}^{-1}$ ). Anaerobic techniques were used throughout all the experiments as previously described (Li et al. 2009). Inoculation and sampling were conducted by using sterile syringes and needles. All trials were conducted in triplicate and the vials were incubated in a BACTRON Anaerobic/Environmental Chamber II (SHELLAB, Sheldon Manufacturing Inc.) at  $30^\circ\text{C}$  in the dark.

## 2.3 Current generation experiment

Current generation was tested using a bioelectrochemical (BEC) reactor that consisted of two identical chambers separated by a cation exchange membrane (Electrolytica Corporation). Each cell chamber had an effective volume of 75 mL. Both electrodes were made of carbon felt ( $4.5 \times 4.5$  cm each, Panex 33 160 K, Zoltek) and set at the bottom of the chamber. Ti wire was inserted inside the carbon felt to connect the circuit. To operate the BEC reactor, a

suspension of *Bacillus* sp. harvested cells (ca.  $10^7$  cells  $\text{mL}^{-1}$ ) and/or metal oxides (including  $\alpha\text{-FeOOH}$ ,  $\gamma\text{-FeOOH}$ ,  $\alpha\text{-Fe}_2\text{O}_3$ ,  $\gamma\text{-Fe}_2\text{O}_3$ ,  $\text{TiO}_2$  and  $\text{Al}_2\text{O}_3$ ,  $4.5 \text{ g L}^{-1}$ ) in the  $\text{NaHCO}_3$  buffered (30 mM, pH 6.8) medium containing glucose (5 mM), was added into the anode chamber under  $\text{N}_2/\text{CO}_2=80:20$  atm. Catholyte containing 0.2 M potassium ferricyanide was added to the cathode chamber under atmospheric pressure. All the experiments were conducted at a controlled temperature of  $30^\circ\text{C}$ . A 1,000  $\Omega$  resistor was used as an external load and cell voltages were recorded by using a 16-channel voltage collection instrument (AD8223, China).

## 2.4 Analytical methods

To determine  $\text{NO}_3^-/\text{NO}_2^-$  and  $\text{NH}_4^+$ , samples were filtrated using a  $0.22 \mu\text{m}$  syringe filter after centrifugation at  $8,500 \times g$  for 20 min to remove the cells and oxides and exposed to  $\text{O}_2$  in order to oxidize Fe(II) rapidly (Weber et al. 2001). The concentration of  $\text{NO}_3^-/\text{NO}_2^-$  was determined by ion chromatography (Dionex ICS-90) with an ion column (IonPac AS14A  $4 \times 250$  mm). The detection limits for both  $\text{NO}_3^-$  and  $\text{NO}_2^-$  was 0.003 mM. A mobile phase consisting of  $\text{Na}_2\text{CO}_3$  (8.0 mM) and  $\text{NaHCO}_3$  (1.0 mM) solution was operated at a flow rate of  $1.0 \text{ mL min}^{-1}$ . The concentration of  $\text{NH}_4^+$  was measured by spectrophotometry at 420 nm after a color reaction with Nessler's reagent (Paul et al. 2007). Before Nessler's reagent was added, an aliquot of the sample to be analyzed was diluted with ultrapure water. Ammonium chloride solutions were used as standards. The HCl-extractable Fe(II) concentrations were determined as previously described (Li et al. 2009). Fe(II) analyses in  $\text{NO}_3^-$  containing samples were performed using a sequential extraction technique (Cooper et al. 2003). The nitrite was removed prior to acidifying the sample to extract adsorbed Fe(II), because nitrite rapidly oxidizes Fe (II) in acidic solution. UV/Vis diffuse-transmittance absorption spectra of the cell suspension of *Bacillus* sp. was measured by an UV/visible spectrophotometer (TU-1901 Beijing, China) equipped with an IS19-1 integrating sphere reflectance attachment. The sample was stored in a  $\text{NaHCO}_3$  buffer solution, and optical length of the cell is 10 mm. The spectrum was taken under aerobic condition.

## 3 Results and discussion

### 3.1 Effects of iron oxides on microbial nitrate/nitrite reduction

Time-dependent nitrate reduction by *Bacillus* sp. in the absence and presence of IOs was shown in Fig. 1a; the calculated first-order reaction rate constant ( $k$ ) was shown in Table 1. The results show that  $\text{NO}_3^-$  was reduced by

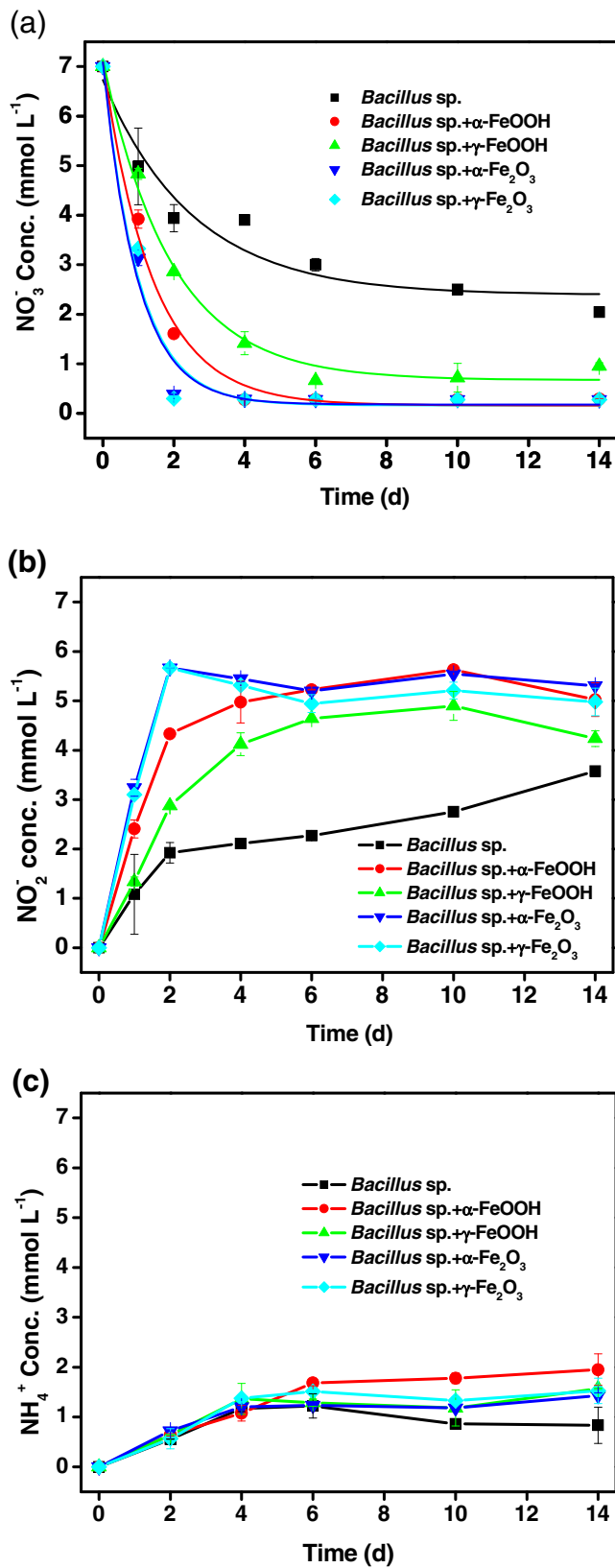


**Fig. 1** a  $\text{NO}_3^-$  reduction, b  $\text{NO}_2^-$  formation, and c  $\text{NH}_4^+$  formation in various experiments with *Bacillus* sp. in the absence or presence of IOs. Initial concentration of  $\text{NO}_3^-$ , 7 mM; *Bacillus* sp.,  $10^7$  cells  $\text{mL}^{-1}$ ; glucose, 5 mM; IOs ( $\alpha\text{-Fe}_2\text{O}_3$ ,  $\alpha\text{-FeOOH}$ ,  $\gamma\text{-FeOOH}$ , and  $\gamma\text{-Fe}_2\text{O}_3$ ), 4.5  $\text{g L}^{-1}$ . The solid line in the first figure is the model-fitted  $\text{NO}_3^-$  curve using the first-order kinetic model, with parameter estimates provided in Table 1. Error bars represent standard deviation of the mean ( $n=3$ )

accelerated markedly in the presence of four iron oxides, and the first-order rate constant was increased to 0.358, 0.493, 0.712, and 0.690  $\text{day}^{-1}$  by the presence of  $\alpha\text{-FeOOH}$ ,  $\gamma\text{-FeOOH}$ ,  $\alpha\text{-Fe}_2\text{O}_3$ , and  $\gamma\text{-Fe}_2\text{O}_3$ , respectively. This indicates that the addition of iron oxides was able to improve the microbial nitrate reduction by *Bacillus* sp. The order of nitrate reduction rates was as follows:  $\alpha\text{-Fe}_2\text{O}_3 > \gamma\text{-Fe}_2\text{O}_3 > \alpha\text{-FeOOH} > \gamma\text{-FeOOH}$ . The major reduced intermediate ( $\text{NO}_2^-$ ) and end products ( $\text{NH}_4^+$ ) were measured as well. As shown in Fig. 1b,  $\text{NO}_2^-$  increased gradually as the  $\text{NO}_3^-$  was reduced, and the  $\text{NO}_2^-$  formation corresponds to the  $\text{NO}_3^-$  reduction in both experiments with *Bacillus* sp. and *Bacillus* sp. + IOs. However, the  $\text{NH}_4^+$  formation (Fig. 1c) in the experiments with *Bacillus* sp. and *Bacillus* sp. + IOs was in a similar concentration levels during the 14 days of incubation.

To clearly verify the difference of nitrate reduction by *Bacillus* sp. with and without IOs, additional experiments

**Table 1** The first-order rate constants of nitrate and nitrite reduction by *Bacillus* sp. in the absence and presence of metal oxides ( $\alpha\text{-Fe}_2\text{O}_3$ ,  $\alpha\text{-FeOOH}$ ,  $\gamma\text{-FeOOH}$ ,  $\gamma\text{-Fe}_2\text{O}_3$ ,  $\text{Al}_2\text{O}_3$  and  $\text{TiO}_2$ ), and by abiotic treatment of  $\text{Fe(II)} + \alpha\text{-FeOOH}$

	$\text{NO}_3^-$ reduction		$\text{NO}_2^-$ reduction	
	$K^a/\text{day}^{-1}$	$R^2$	$k/\text{day}^{-1}$	$R^2$
<i>Bacillus</i> sp.	$0.273 \pm 0.083^b$	0.946	$0.021 \pm 0.007$	0.876
<i>Bacillus</i> sp. + $\alpha\text{-FeOOH}$	$0.493 \pm 0.050$	0.993	$0.040 \pm 0.005$	0.976
<i>Bacillus</i> sp. + $\gamma\text{-FeOOH}$	$0.358 \pm 0.040$	0.992	$0.036 \pm 0.008$	0.871
<i>Bacillus</i> sp. + $\alpha\text{-Fe}_2\text{O}_3$	$0.712 \pm 0.119$	0.982	$0.047 \pm 0.007$	0.939
<i>Bacillus</i> sp. + $\gamma\text{-Fe}_2\text{O}_3$	$0.690 \pm 0.137$	0.974	$0.043 \pm 0.004$	0.975
<i>Bacillus</i> sp. + $\text{TiO}_2$	$0.400 \pm 0.040$	0.993	$0.034 \pm 0.008$	0.946
<i>Bacillus</i> sp. + $\text{Al}_2\text{O}_3$	$0.509 \pm 0.028$	0.998	$0.045 \pm 0.006$	0.982
$\text{Fe(II)} + \alpha\text{-FeOOH}$	$0.027 \pm 0.007$	0.996	$0.008 \pm 0.002$	0.892

Initial concentration of  $\text{NO}_3^-$ , 7 mM; *Bacillus* sp.,  $10^7$  cells  $\text{mL}^{-1}$ ; glucose, 5 mM; metal oxides, 4.5  $\text{g L}^{-1}$ ;  $\text{Fe}^{2+}$  0.7 mM

<sup>a</sup> The first-order rate coefficients of nitrate and nitrite reduction

<sup>b</sup> Error for the nitrate/nitrite reduction rate constants indicate the standard deviation of the slope of the linear regression equation for the nitrate/nitrite concentration vs. time plot over 14 days incubation

*Bacillus* sp. incompletely after 14 days of incubation ( $k=0.273 \text{ day}^{-1}$ ). In the first 4 days, the  $\text{NO}_3^-$  reduction was

were conducted using nitrite instead of nitrate, as *Bacillus* sp. can also reduce the nitrate reduction product, nitrite (Espinosa-de-los-Monteros and Martinez 2001; Dou et al. 2010; Rajakumar et al. 2008). Compared to the nitrate reduction, less than 22% of the initial nitrite was reduced by *Bacillus* sp. after 14 days of incubation, and the first-order rate constant of nitrite reduction by *Bacillus* sp. was only  $0.021 \text{ day}^{-1}$  (see Table 1). Similar to the case of nitrate reduction,  $\text{NO}_2^-$  reduction by *Bacillus* sp. was also accelerated in the presence of IOs (Fig. 2a), wherein the  $k$  value was raised to 0.040, 0.043, 0.047, and  $0.036 \text{ day}^{-1}$  by the presence of  $\alpha\text{-FeOOH}$ ,  $\gamma\text{-FeOOH}$ ,  $\alpha\text{-Fe}_2\text{O}_3$ , and  $\gamma\text{-Fe}_2\text{O}_3$ , respectively. In addition, the  $\text{NH}_4^+$  formation (Fig. 2b) was coincidental

to the nitrite reduction. These results, accompanying those of  $\text{NO}_3^-$  reduction, confirm that *Bacillus* sp. was able to reduce  $\text{NO}_3^-$  via  $\text{NO}_2^-$  to  $\text{NH}_4^+$ , and the presence of four IOs could accelerate both the nitrate and nitrite reduction by *Bacillus* sp.

### 3.2 Role of Fe(II) during nitrate/nitrite reduction with *Bacillus* sp. and IOs

Since *Bacillus* sp. can reduce IOs under anoxic condition (Kanso et al. 2002; Boone et al. 1995; Cheng and Li 2009; Pollock et al. 2007), three experiments of *Bacillus* sp. + IOs (i.e., with and without  $\text{NO}_3^-/\text{NO}_2^-$ ) were conducted to evaluate the Fe(II) formation during the incubation. As shown in Fig. 3, the HCl-extractable Fe(II) concentrations in the *Bacillus* sp. + IOs with  $\text{NO}_3^-$  were similar with those in the *Bacillus* sp. + IOs with  $\text{NO}_2^-$ , both of which were significantly less than those in the *Bacillus* sp. + IOs experiment without  $\text{NO}_3^-/\text{NO}_2^-$ . The iron reduction amounts produced by *Bacillus* sp. without  $\text{NO}_3^-/\text{NO}_2^-$  were ranked as  $\gamma\text{-FeOOH} > \alpha\text{-FeOOH} > \alpha\text{-Fe}_2\text{O}_3 \approx \gamma\text{-Fe}_2\text{O}_3$ , which was strongly correlated to the order of surface area as  $\alpha\text{-FeOOH}$  ( $121 \text{ m}^2 \text{ g}^{-1}$ )  $\approx \gamma\text{-FeOOH}$  ( $115 \text{ m}^2 \text{ g}^{-1}$ )  $> \alpha\text{-Fe}_2\text{O}_3$  ( $29.4 \text{ m}^2 \text{ g}^{-1}$ )  $> \gamma\text{-Fe}_2\text{O}_3$  ( $14.36 \text{ m}^2 \text{ g}^{-1}$ ), and the order of Fe(III) available as  $\gamma\text{-FeOOH}$  ( $12.8 \text{ mmol mmol}^{-1}$ )  $> \alpha\text{-FeOOH}$  ( $5.57 \text{ mmol mmol}^{-1}$ )  $> \alpha\text{-Fe}_2\text{O}_3$  ( $0.904 \text{ mmol mmol}^{-1}$ )  $> \gamma\text{-Fe}_2\text{O}_3$  ( $0.676 \text{ mmol mmol}^{-1}$ ) as previously reported (Liu et al. 2011; Li et al. 2011).

When IOs were served as electron acceptor, no noticeable increases in the cell numbers were observed in all biotic experiments in this study (data not shown). *Bacillus* sp. is a fermentative bacterium that reduces relatively trivial amounts of Fe(III) to achieve a more favorable electron balance during fermentation of glucose, so it is unlikely for *Bacillus* sp. to gain energy for its growth when Fe(III) oxide serves as an electron acceptor (Kanso et al. 2002; Boone et al. 1995; Cheng and Li 2009; Pollock et al. 2007). The results of this study show that the bacterium produced only approximately 0.48–1.0 mM of HCl-extractable Fe(II) after 14 day of incubation in the *Bacillus* sp. + IOs without  $\text{NO}_3^-/\text{NO}_2^-$ , and more than 77% of the HCl-extractable Fe(II) was determined as adsorbed Fe(II). The lower level of Fe(II) formation in the *Bacillus* sp. + IOs experiments with  $\text{NO}_3^-/\text{NO}_2^-$  may be due to the competition of nitrate/nitrite reduction and Fe(III) reduction because both nitrate/nitrite and Fe(III) oxides can be reduced by *Bacillus* sp. And inhibition of Fe(III) reduction in the presence of nitrate has been reported in some studies of fermentative Fe(III)-reducing microorganisms (Lovley et al. 2004).

Nevertheless, it is necessary to evaluate the role of Fe(II) species potentially produced by *Bacillus* sp., because Fe(II), which was associated with iron mineral surface (e.g., goethite and green rust), was subject to abiotic reduction of  $\text{NO}_3^-$  (Ottley et al. 1997; Wang et al. 2008). Three abiotic

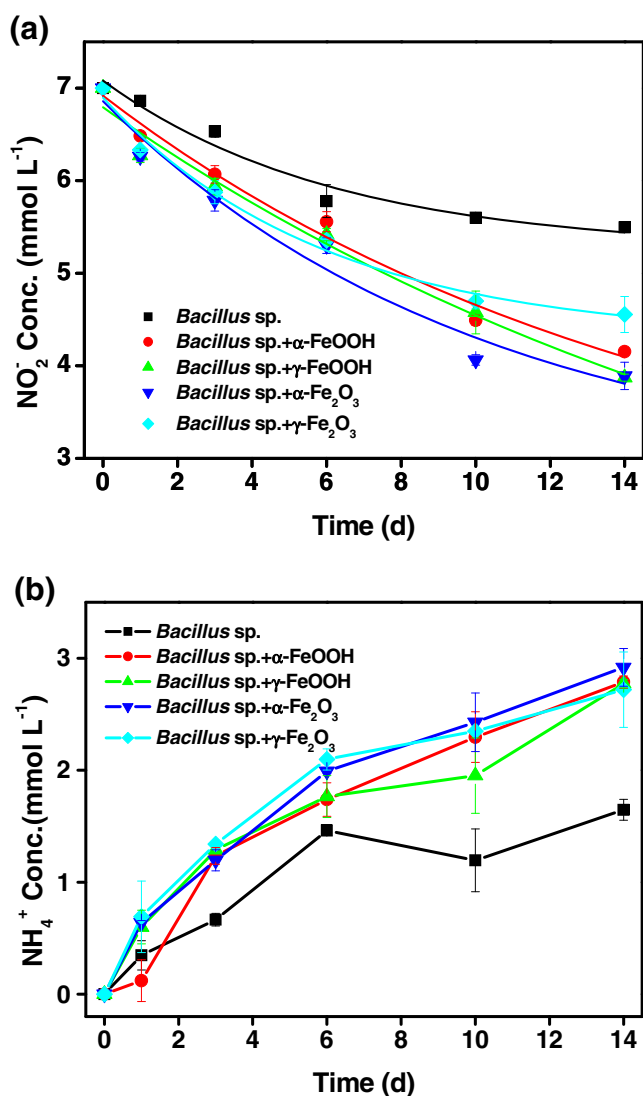
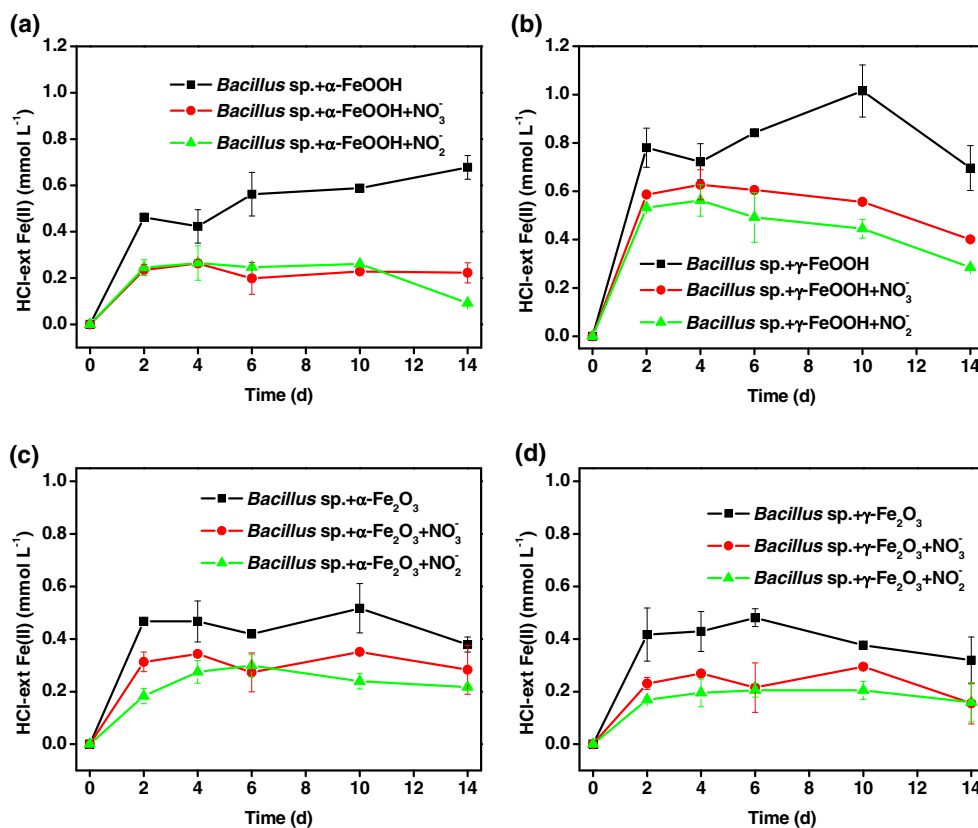


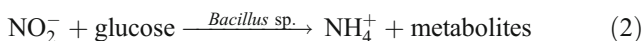
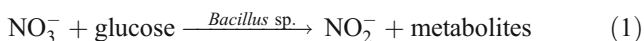
**Fig. 2** a  $\text{NO}_2^-$  reduction and b  $\text{NH}_4^+$  formation in various systems with *Bacillus* sp. in the absence or presence of IOs. Initial concentration of  $\text{NO}_2^-$ , 7 mM; *Bacillus* sp.,  $10^7$  cells  $\text{mL}^{-1}$ ; glucose, 5 mM; IOs,  $4.5 \text{ g L}^{-1}$ . The solid line in the first figure is the model-fitted  $\text{NO}_2^-$  curve using the first-order kinetic model, with parameter estimates provided in Table 1. Error bars represent standard deviation of the mean ( $n=3$ )

**Fig. 3** Total Fe(II) (HCl-extractable Fe(II)) formation in various experiments including *Bacillus* sp. + IOs, *Bacillus* sp.+IOs+NO<sub>3</sub><sup>-</sup> and *Bacillus* sp.+IOs+NO<sub>2</sub><sup>-</sup>. **a** α-FeOOH, **b** γ-FeOOH, **c** α-Fe<sub>2</sub>O<sub>3</sub>, and **d** γ-Fe<sub>2</sub>O<sub>3</sub>. Initial concentration of NO<sub>3</sub><sup>-</sup>/NO<sub>2</sub><sup>-</sup>, 7 mM; *Bacillus* sp., 10<sup>7</sup> cells mL<sup>-1</sup>; glucose, 5 mM; IOs, 4.5 g L<sup>-1</sup>. Error bars represent standard deviation of the mean (n=3)



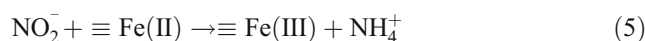
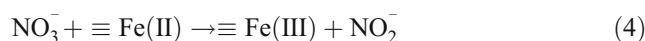
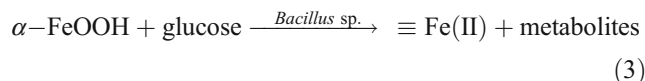
experiments of Fe(II), α-FeOOH, and Fe(II) + α-FeOOH were tested for NO<sub>3</sub><sup>-</sup>/NO<sub>2</sub><sup>-</sup> reduction. As presented in Figs. 4a and 5a, no NO<sub>3</sub><sup>-</sup>/NO<sub>2</sub><sup>-</sup> reduction was observed in ferrous ion or α-FeOOH experiment, and the NO<sub>3</sub><sup>-</sup>/NO<sub>2</sub><sup>-</sup> was reduced very slowly in the Fe(II) + α-FeOOH experiment. Merely 12% of the initial NO<sub>3</sub><sup>-</sup> and 5% of the initial NO<sub>2</sub><sup>-</sup> was reduced at the end of experiment in the Fe(II) + α-FeOOH experiment, which was less than that in the *Bacillus* sp. experiment. However, no significant NH<sub>4</sub><sup>+</sup> was detected in the Fe(II) + α-FeOOH experiment with NO<sub>3</sub><sup>-</sup>/NO<sub>2</sub><sup>-</sup>, which indicated that NH<sub>4</sub><sup>+</sup> formation was mainly from the microbial activity of *Bacillus* sp.

Herein, the reaction kinetic of nitrate and nitrite reduction by *Bacillus* sp. in the presence of α-FeOOH was analyzed as follows. The reactions (1) and (2) show the direct nitrate and nitrite reduction to nitrite and ammonium by *Bacillus* sp. with glucose, respectively. As shown in Table 1, the first-order rate constant of nitrate (*k*<sub>1, nitrate</sub>) and nitrite (*k*<sub>2, nitrite</sub>) reduction by *Bacillus* sp. as reactions (1) and (2) was 0.273 and 0.021 day<sup>-1</sup>, respectively.



In the presence of α-FeOOH, besides reactions (1) and (2), iron reduction by *Bacillus* sp. (reaction 3) and chemical

nitrate and nitrite reductions by adsorbed ferrous species (reactions iv and v) can take place in sequence. According to the results in Fig. 3a, the zero-order rate of α-FeOOH reduction by *Bacillus* sp. (*r*<sub>3</sub>) as reaction (3) was 0.037 mmol L<sup>-1</sup> day<sup>-1</sup>. The first-order rate constant of nitrate (*k*<sub>4, nitrate</sub>) and nitrite (*k*<sub>5, nitrite</sub>) reduction by adsorbed Fe(II) on α-FeOOH as reactions (4) and (5) was 0.027 and 0.008 day<sup>-1</sup>, respectively, either of which was evidently lower than that by *Bacillus* sp..



In nitrate reduction experiments, α-FeOOH could serve as competitive electron acceptor for nitrate reduction by *Bacillus* sp.. The nitrate reduction could be divided into two pathways, wherein one is reaction (1) and the other is reactions (3) and (4). Nitrate reduction by *Bacillus* sp. was indicated to be faster than that by adsorbed Fe(II) on α-FeOOH, and the latter was limited by the low rate of iron reduction by *Bacillus* sp. As a result, nitrate reduction by *Bacillus* sp. was supposed to be slow down in the presence

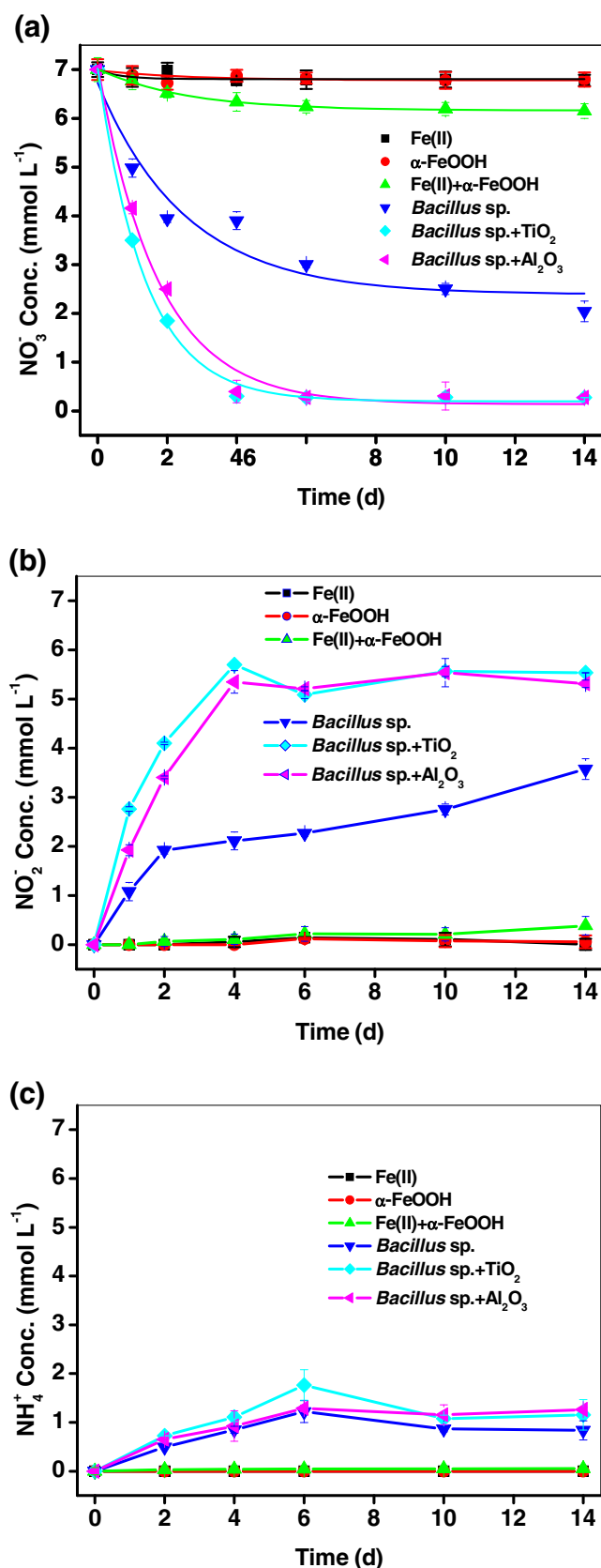


**Fig. 4** a NO<sub>3</sub><sup>-</sup> reduction, b NO<sub>2</sub><sup>-</sup> formation, and c NH<sub>4</sub><sup>+</sup> formation in various experiments. Initial concentration of NO<sub>3</sub><sup>-</sup>, 7 mM; *Bacillus* sp., 10<sup>7</sup> cells mL<sup>-1</sup>; glucose, 5 mM; non-Fe oxides (Al<sub>2</sub>O<sub>3</sub> and TiO<sub>2</sub>), 4.5 g L<sup>-1</sup>; Fe<sup>2+</sup>, 0.7 mM. The solid line in the first figure is the model-fitted NO<sub>3</sub><sup>-</sup> curve using the first-order kinetic model, with parameter estimates provided in Table 1. Error bars represent standard deviation of the mean ( $n=3$ )

of  $\alpha$ -FeOOH. However, the finding that the IOs could accelerate the nitrate and nitrite reduction by *Bacillus* sp. may not be mainly due to the chemical reduction by the biogenic adsorbed Fe(II), but some other factors.

### 3.3 Effects of non-Fe oxides on microbial nitrate/nitrite reduction

Fe(II) produced by microorganisms was reported to be reoxidized to Fe(III) with nitrate serving as the electron acceptor (Finneran et al. 2002; Jørgensen et al. 2009). To avoid the potential effects of biogenic Fe(II) on nitrate reduction, mainly chemical reduction by adsorbed Fe(II) on surface of IOs, Al<sub>2</sub>O<sub>3</sub> and TiO<sub>2</sub>, as non-Fe oxides, were added with equivalent quantity into the cell suspension instead of iron oxides. The results in Figs. 4a and 5a showed that both Al<sub>2</sub>O<sub>3</sub> and TiO<sub>2</sub> accelerated the NO<sub>3</sub><sup>-</sup> and NO<sub>2</sub><sup>-</sup> reduction by *Bacillus* sp., and increased the corresponding reduction rates to 0.400 and 0.509 day<sup>-1</sup> for nitrate reduction, respectively, as well as 0.034 and 0.045 day<sup>-1</sup> for nitrite reduction. These results suggest that adding non-iron oxides can also result in accelerated microbial NO<sub>3</sub><sup>-</sup>/NO<sub>2</sub><sup>-</sup> reduction by *Bacillus* sp. Both the results of iron oxides and non-iron oxides suggest that the acceleration of nitrate and nitrite reduction was not predominantly attributed to the biogenic ferrous species, but to some other unrecognized factors.

### 3.4 Effects of iron oxides and non-Fe oxides on current generation

Nitrate/nitrite, as a soluble electron acceptor for reduction by *Bacillus* sp., can easily enter the cell to be reduced in the cytoplasm. However, iron oxides, as an insoluble electron acceptor, mainly participate or influence the extracellular electron transfer process of microorganisms. Thus, it was difficult to distinguish whether the iron oxides are able to influence the extracellular or intracellular reduction of nitrate. Previously, *S. putrefaciens* was thought to be able to reduce electrode to produce electricity in MFCs (Kim et al. 1999). Bond and Lovley (2003) suggested that the electrode surfaces were serving as terminal electron acceptors for *Geobacteraceae* and they can better understand this electron transfer process for energy production. Similarly, the fermentative microorganisms, such as *Klebsiella* sp.,

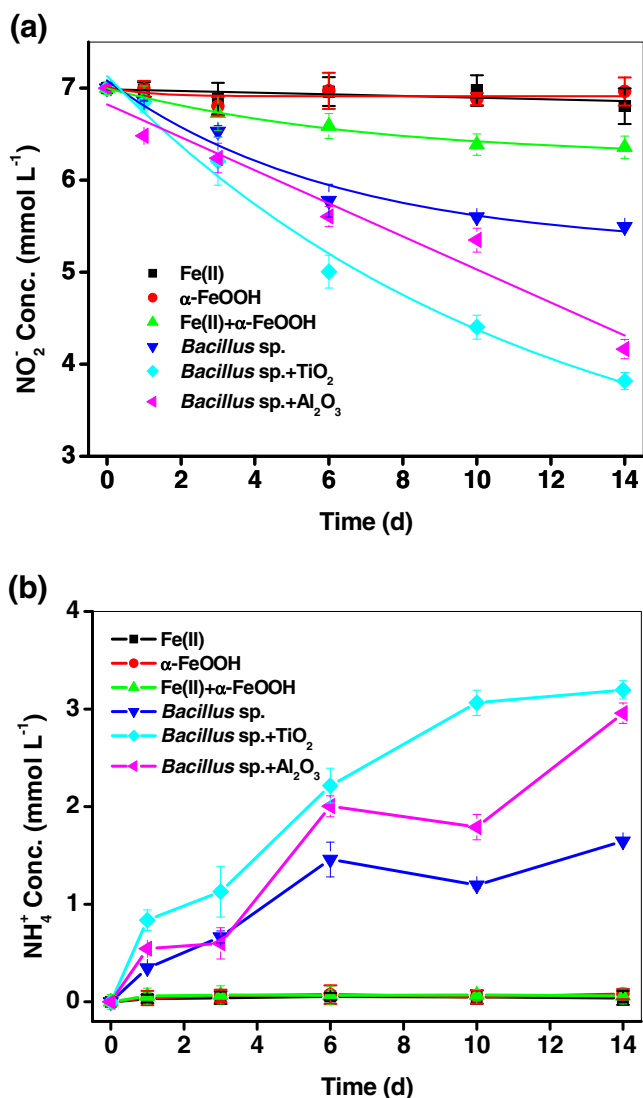


**Fig. 5** **a**  $\text{NO}_2^-$  reduction and **b**  $\text{NH}_4^+$  formation in various abiotic system of Fe(II),  $\alpha$ -FeOOH, and Fe(II) +  $\alpha$ -FeOOH and various biotic systems with *Bacillus sp.* in the absence or presence of non-Fe oxides. Initial concentration of  $\text{NO}_2^-$ , 7 mM; *Bacillus sp.*,  $10^7$  cells mL<sup>-1</sup>; glucose, 5 mM; non-Fe oxides (Al<sub>2</sub>O<sub>3</sub> and TiO<sub>2</sub>), 4.5 g L<sup>-1</sup>; Fe(II), 0.7 mM. The solid line in the first figure is the model-fitted  $\text{NO}_2^-$  curve using the first-order kinetic model, with parameter estimates provided in Table 1. Error bars represent standard deviation of the mean ( $n=3$ )

*Escherichia coli*, and *Bacillus sp.* have also been demonstrated to be capable of using the anode as an electron acceptor under anaerobic condition in the MFCs (Xia et al. 2010; Zhang et al. 2011; Nimje et al. 2009; Choi et al. 2001). The anodes in MFCs have been used as an important solid substrate to investigate the extracellular electron transfer of microorganisms (Rabaey and Verstraete 2005). In this study, we established a BEC reactor to study the anode reduction by *Bacillus sp.* in the presence of different iron oxides.

As presented in Fig. 6a, the current generation in the reactor inoculated with *Bacillus sp.* increased to the highest

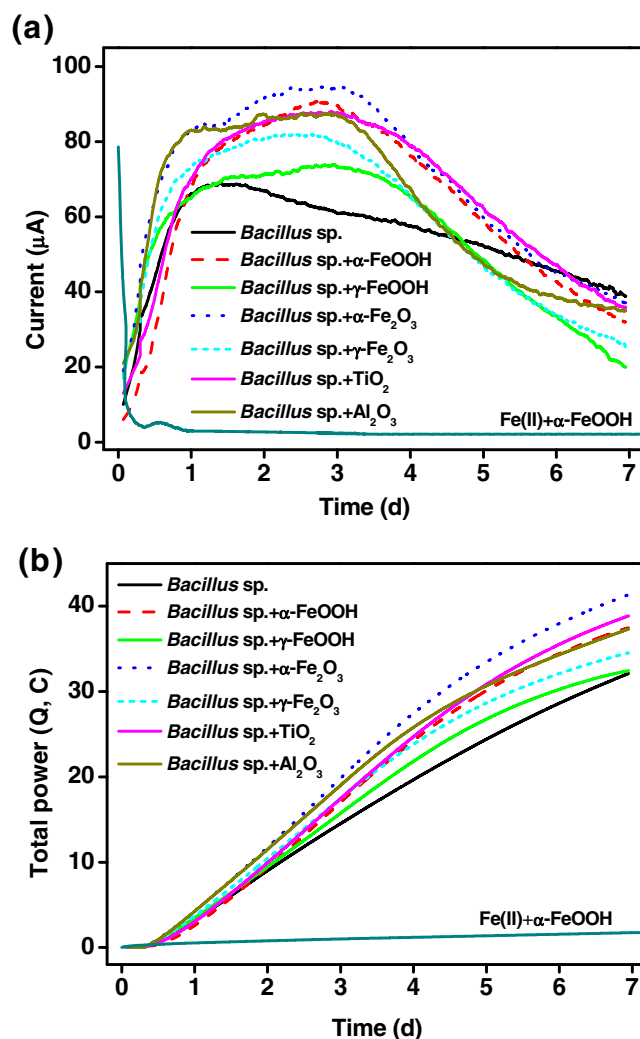


**Fig. 6** **a** Current generation in various experiments in the microbial electrochemical cell (initial concentration of *Bacillus sp.*,  $10^7$  cells mL<sup>-1</sup>; glucose, 5 mM; metal oxides ( $\alpha$ -Fe<sub>2</sub>O<sub>3</sub>,  $\alpha$ -FeOOH,  $\gamma$ -FeOOH,  $\gamma$ -Fe<sub>2</sub>O<sub>3</sub>, Al<sub>2</sub>O<sub>3</sub>, and TiO<sub>2</sub>), 4.5 g L<sup>-1</sup>, Fe(II) (0.7 mM)+ $\alpha$ -FeOOH) (4.5 g L<sup>-1</sup>), and **b** the calculated total power outputs in various systems

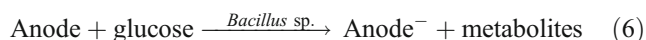
output at 68  $\mu\text{A}$  after 1 day, and then decreased gradually. The highest current output was observed as 90, 74, 95, and 82  $\mu\text{A}$ , in the reactors with *Bacillus sp.* in the presence of  $\alpha$ -FeOOH,  $\gamma$ -FeOOH,  $\alpha$ -Fe<sub>2</sub>O<sub>3</sub>, and  $\gamma$ -Fe<sub>2</sub>O<sub>3</sub>, respectively. In order to clearly evaluate the acceleration effect of IOs on the current generation by *Bacillus sp.*, the total power outputs (Q) with time dependence during the incubation were calculated. The results in Fig. 6b confirm that all reactors with *Bacillus sp.* + IOs had higher power output than the *Bacillus sp.* alone. As a result, it was demonstrated that the addition of IOs could increase the current and power outputs by *Bacillus sp.*

The current generation was reported to be a consequence of the microbial activity of *Bacillus sp.* (Nimje et al. 2009; Choi et al. 2001). The *Bacillus sp.* biofilm established on the

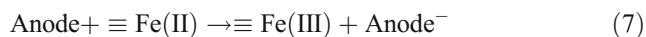


anode is the key factor for extracellular electron transfer from *Bacillus* sp. to the anode in the BEC. In this study, a thick layer composed of cells and IOs was observed in the suspension containing *Bacillus* sp. and IOs. However, the precipitation of IOs and combination of IOs and cells on the surface of the anode may decrease the surface sites for the direct attachment of cells. This would reduce the direct electron transfer from cell to the electrode and thereby lower the current generation, which was contrary to our finding.

Since both anode and Fe(III) oxides are insoluble electron acceptors for *Bacillus* sp., anode and iron reductions may take place simultaneously. To illustrate the potential effect of Fe(II) produced by *Bacillus* sp., the abiotic experiments with ferrous ion and Fe(II) +  $\alpha$ -FeOOH were conducted for current generation as well. Current output in the ferrous ion experiment was less than 1  $\mu$ A throughout the incubation (data not shown), while that in the Fe(II) +  $\alpha$ -FeOOH experiment was high (78.6  $\mu$ A) at the beginning, and then decreased sharply to lower than 10  $\mu$ A after 5 min (see Fig. 6a). The current generation by Fe(II) +  $\alpha$ -FeOOH in MFCs was mainly due to the electron transfer from Fe(II) to anode, as a result of the reduction of Fe(II) to Fe(III). The high current at the beginning and quick decrease of current suggested that the electron transfer rate from Fe(II) to anode was very fast and instantaneous. In order to illustrate clearly the contributions of *Bacillus* sp. and adsorbed Fe(II) on current generation, their reaction kinetics was analyzed in detail as below. First, the anode can be reduced directly by *Bacillus* sp. (reaction 6). *Bacillus*



Chemical current generation by the adsorbed Fe(II) (reaction 7) followed the microbial iron reduction by *Bacillus* sp. in the presence of  $\alpha$ -FeOOH (reactions 3).



According to the current and power outputs in Fig. 6, the anode reduction rate of reaction (6) was evidently faster than that of reactions (3), so the presence of IOs is supposed to inhibit the current generation by *Bacillus* sp. The anode reduction rate of reaction (7) was fast and instantaneous, but the Fe(II) formation was restricted by the low rate of reaction (3). Consequently, even though Fe(II) can be produced by *Bacillus* sp., such slow Fe(II) formation can not afford continuous enhanced effect on the current generation. Obviously, the Fe(II) produced by *Bacillus* sp. cannot support the fact that IOs accelerated the microbial current generation.

Moreover,  $\text{Al}_2\text{O}_3$  and  $\text{TiO}_2$ , instead of iron oxides, were added into the *Bacillus* sp. suspension in the electrochemical cell to avoid the effect of Fe(II) on the current generation. Similarly, the current and power outputs by *Bacillus* sp.

were enhanced by the presence of these non-Fe oxides (see Fig. 6). Herein, some unknown mechanisms need further exploration. It was reported that the addition of  $\alpha$ - $\text{Fe}_2\text{O}_3$  colloids increases the current generation of *Shewanella loihica* PV-4 (Nakamura et al. 2009a), and the authors proposed that the  $\alpha$ - $\text{Fe}_2\text{O}_3$  nanocolloids would force the cells to self-assemble into an interconnected bacterial network for promoting a long-distance extracellular electron transfer process to the electrode surface. Similarly, such bacterial network with IOs was presumed to responsible for the enhanced microbial current generation by IOs, which would be elucidated in detail as follow.

### 3.5 Elucidation for the interaction mechanism among *Bacillus* sp., IOs, and electron acceptors

The present study has clearly demonstrated that the nitrate and current generation were directly attributed to the microbial activity of *Bacillus* sp., both of which could be enhanced in the presence of IOs. The fact that such acceleration caused by the IOs surpassed the contribution of biogenic Fe(II) suggests that there might be some unrecognized mechanisms.

It has been indicated that c-type cytochrome (c-Cyt) in outer membrane of iron-reducing bacteria (e.g., *Shewanella* and *Geobacter* species) can mediate electron transfer from cell to attached iron oxide in cellular metabolism; this electron transfer results in iron reduction and current generation (Hernandez and Newman 2001). In the c-Cyt, heme acts as an active center of electron transport chain, therefore, electron transport from bacteria to metal oxides is attributed to electron transfer between heme and iron oxide (Mori et al. 2011). Clear evidence for conduction band-mediated electron transfer between heme and semiconductor  $\text{TiO}_2$  was obtained from a spectroelectrochemical analysis (Staniszewski et al. 2007). Similarly, iron oxides were also semiconductors (Xu and Schoonen 2000) and can also be explained by a conduction band mediated processes. When the IOs come in contact with cells, an electron transfer process would take place between the iron oxides' conduction band (IOs' CB) and outer membrane enzyme (OME) if the redox potential of the OME was more negative than that of the IO's CB. This phenomenon has been extensively studied in the electrochemistry of semiconductors (Yang et al. 2010; Xu and Schoonen 2000). In this study, the diffuse transmittance absorption was used to measure the cell suspension of *Bacillus* sp., and it was found that the absorption spectra of some c-Cyt like species according to the peak at 413 nm (Fig. 7), which was near to the c-Cyt at 410–419 nm in the other's research (Nakamura et al. 2009b). This might be an indicator of heme species of OME in *Bacillus* sp. The redox potential of the OME of some strains has been reported as lower than  $-0.2$  V (Thauer et al. 1977; Nakamura et al. 2009a). Xu and Schoonen (2000) reported that the normal hydrogen

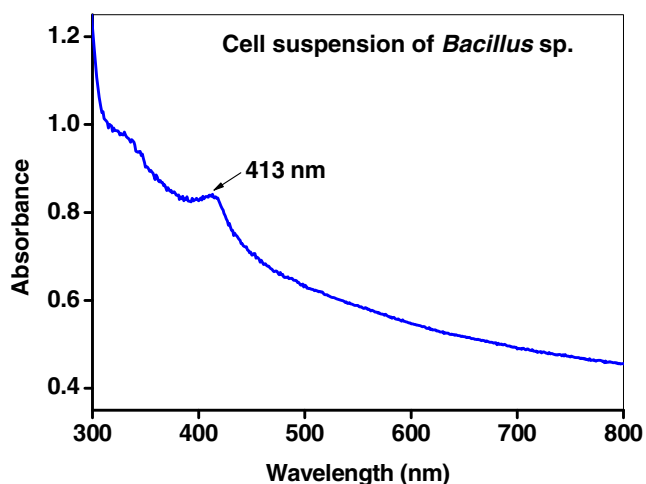


**Fig. 7** UV/vis diffuse-transmittance absorption spectra of the cell suspension of *Bacillus* sp. in a NaHCO<sub>3</sub> buffer solution (OD<sub>600</sub>=2.1), and optical length of the cell is 10 mm. The spectrum was taken under aerobic condition

electrode (NHE, pH 7) of CB is -0.133 V and +0.167 V for Fe<sub>2</sub>O<sub>3</sub> and FeOOH, respectively. Hence, no energy barrier for the electron exchange appears between the OME and the IOs' CB. In addition, the redox potential of NO<sub>3</sub><sup>-</sup>/NO<sub>2</sub><sup>-</sup> is +0.43 V at pH 7 (Beller 2005), and the NHE of graphite anode was often poised at around +0.50 V (Holmes et al. 2004). Similarly, the electron transfer process can also take place between the IOs' CB and nitrate or electrode. In summary, an energy gradient, from the order of redox potential ranking as OME < IOs' CB < nitrate or electrode could provide a continuous driving force for the electrons to be transferred from the cell to IOs to terminal electron acceptors (nitrate or electrode). Furthermore, It was also reported that the electron injection from heme into conduction band of semiconductors was very fast, which may lead a fast trapping by other electrons acceptors (e.g., nitrate, organic halides, and electrode; Mimica et al. 2001; Obare et al. 2003; Stromberg et al. 2006; Hoffmann et al. 1995). As a result, the enhancement on nitrate reduction and current generation might be a consequence of the fast electron transfer from the OME to the IOs' CB to the terminal electron acceptors (nitrate or electrode).

As discussed above, three ways for nitrate reduction and current generation in the interaction system of *Bacillus* sp. and IOs are possible: (1) direct enzymatic reduction by *Bacillus* sp., (2) reduction by the biogenic adsorbed Fe(II), and (3) conduction band of iron oxides-mediated electron transfer from *Bacillus* sp. to the electron acceptors. The possible electron transport way was proposed in Fig. 8.

### 3.6 Environmental implication

In the anoxic natural environment, IOs can coexist with many substrates (or electron acceptors), e.g., nitrate, sulfate,

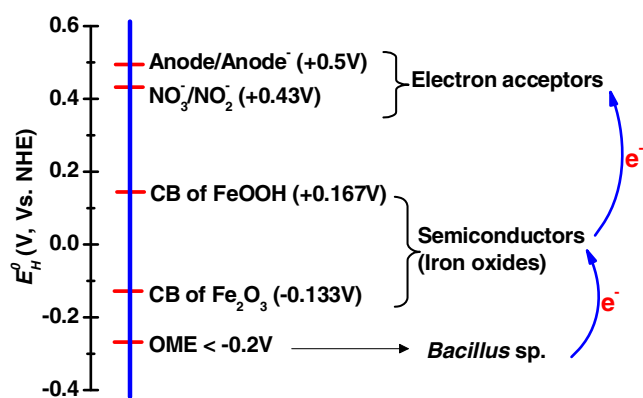


**Fig. 8** Proposed mechanism of iron based semiconductor mediating electron transfer from *Bacillus* sp. to NO<sub>3</sub><sup>-</sup> and anode on a basis of the different redox potentials for outer membrane enzyme (OME) of *Bacillus* sp., conduction band (CB) of IOs, and electron acceptors (nitrate and anode)

and humic substances. Among these substrates, the nitrate reductions are predominantly subject to microbial activity (Moreno-Vivián et al. 1999; Cabello et al. 2004; Gonzalez et al. 2006). In the presence of soluble Fe(III) species, e.g., Fe (III) citrate, Fe(III) phosphate and Fe(III)EDTA, microbial nitrate and Fe(III) reductions occur simultaneously (DiChristina 1992; Obuekwe and Westlake 1982). However, Cooper et al. (2003) found that no significant Fe(III) reduction occurs until nitrate and nitrite has been exhausted when solid phase, Fe(III) oxide minerals is served as the Fe(III) source for *S. putrefaciens* 200, and the goethite also results in a significant decrease in the rates of microbial nitrate and nitrite reductions.

In the present study, *Bacillus* sp. was proved to be with relatively weak Fe(III) oxide reduction and strong nitrate reduction abilities, and the presence of IOs evidently accelerated the nitrate reduction by *Bacillus* sp. Though the Fe(II) adsorbed on the goethite surface has been demonstrated to drive slow NO<sub>3</sub><sup>-</sup> reduction (Hansen et al. 1996), however, the IOs were suggested to inhibit the microbial nitrate reduction because the nitrate reduction rate of biotic–abiotic reactions (i.e., the microbial iron reduction and chemical reduction by adsorbed ferrous) is usually lower than that of direct biotic reduction by bacteria (Straub et al. 1996; Weber et al. 2001). To our knowledge, this was the first case to report the enhanced effect of IOs on the nitrate and nitrite reductions by the fermentor, *Bacillus* sp. This result may help to extend the understanding of nitrate and nitrite reductions in the natural environment with fermentative bacteria and iron-bearing minerals.

Artificial anode may not coexist with Fe(III) oxides in the natural environment, but many DIRB and fermentative bacteria have been used to demonstrate the ability of current generation through different electron transfer pathways in the electrochemical cells. The finding that the IOs can

facilitate the current generation by *Bacillus* sp. in the BEC reactor can provide a framework of the possible reactions that occurred in our experiments of nitrate reduction and current generation. The proposed mechanism that the electron can be transferred extracellularly from the OME to the IOs' CB to the terminal electron acceptor remains quite speculative, and further study needs to identify the electrochemical and biochemical properties of responsible OME in *Bacillus* sp., and to understand the electron exchange between bacteria and a wide range of coexisting electron acceptors in the presence of IOs.

#### 4 Conclusions

The inhibition of microbial reduction of nitrate, nitrite, and current generation in the presence of Fe(III) oxides as a strictly competitive electron acceptor has been previously reported. However, our current results showed that iron oxides obviously enhanced the nitrate/nitrite reduction and current generation by *Bacillus* sp. Nitrate/nitrite reduction by the biogenic Fe(II) on the oxide surface was proven to have taken place, but it showed lower reduction rates than direct nitrate/nitrite reduction and current generation by *Bacillus* sp., which may lead the inhibitory effects for nitrate/nitrite reduction and current generation. Interesting, the presence of four types of iron oxides and even the non-iron oxides as comparing samples, all enhanced nitrate/nitrite reduction and current generation by *Bacillus* sp. Based on the redox potential of *Bacillus* sp., conduction band of iron oxides, and electron acceptors, the role of iron oxide during nitrate/nitrite reduction and current generation was speculated as a conduction band of iron oxides mediating the electron transfer from *Bacillus* sp. to nitrate/nitrite and anode. The current findings provide new insights into microbial reduction of coexisting substrates under anoxic environments.

**Acknowledgments** The authors would thank the National Natural Science Foundations of China (no. 40901114, 41025003, and 41101217), "973" Program (no. 2010CB134508), Excellent Young Scientist Foundation in Guangdong Academy of Sciences (2010), China Postdoctoral Science Foundation (no. 2011M501104), and Natural Science Foundation of Guangdong Province (no. S2011040001094) for financial support.

#### References

- Behrends T, Van Cappellen P (2005) Competition between enzymatic and abiotic reduction of uranium(VI) under iron reducing conditions. *Chem Geol* 220:315–327
- Beller HR (2005) Anaerobic, Nitrate-dependent oxidation of U(IV) oxide minerals by the chemolithoautotrophic bacterium *Thiobacillus denitrificans*. *Appl Environ Microbiol* 71:2170–2174
- Bond DR, Lovley DR (2003) Electricity production by *Geobacter sulfurreducens* attached to electrodes. *Appl Environ Microbiol* 69:1548–1555
- Boone DR, Liu Y, Zhao ZJ, Balkwill DL, Drake GR, Stevens TO, Aldrich HC (1995) *Bacillus infernus* sp. nov., an Fe(III)- and Mn(IV)-reducing anaerobe from the deep terrestrial subsurface. *Int J Syst Bacteriol* 45:441–448
- Borch T, Kretzschmar R, Kappler A, Cappellen PV, Ginder-Vogel M, Voegelin A, Campbell K (2010) Biogeochemical redox processes and their impact on contaminant dynamics. *Environ Sci Technol* 44:15–23
- Cabello P, Roldan MD, Moreno-Vivian C (2004) Nitrate reduction and the nitrogen cycle in archaea. *Microbiology* 150:3527–3546
- Cheng GJ, Li XH (2009) Bioreduction of chromium (VI) by *Bacillus* sp. isolated from soils of iron mineral area. *Eur J Soil Biol* 45:483–487
- Choi Y, Song JY, Jung S, Kim S (2001) Optimization of the performance of microbial fuel cells containing alkalophilic *Bacillus* sp. *J Microbiol Biotechnol* 11:863–869
- Coby AJ, Picardal FW (2005) Inhibition of NO<sub>3</sub><sup>-</sup> and NO<sub>2</sub><sup>-</sup> by microbial Fe(III) reduction: evidence of a reaction between NO<sub>2</sub><sup>-</sup> and cell surface-bound Fe<sup>2+</sup>. *Appl Environ Microbiol* 71:5267–5274
- Cooper DC, Picardal FW, Schimmelmann A, Coby AJ (2003) Chemical and biological interactions during nitrate and goethite reduction by *Shewanella putrefaciens* 200. *Appl Environ Microbiol* 69:3517–3525
- DiChristina TJ (1992) Effects of nitrate and nitrite on dissimilatory iron reduction by *Shewanella putrefaciens* 200. *J Bacteriol* 174:1891–1896
- Dou J, Ding A, Liu X, Du Y, Deng D, Wang J (2010) Anaerobic benzene biodegradation by a pure bacterial culture of *Bacillus cereus* under nitrate reducing conditions. *J Environ Sci (China)* 22:709–715
- Espinosa-de-los-Monteros J, Martinez A, Valle F (2001) Metabolic profiles and *aprE* expression in anaerobic cultures of *Bacillus subtilis* using nitrate as terminal electron acceptor. *Appl Microbiol Biotechnol* 57:379–384
- Finneran KT, Housewright MR, Lovley DR (2002) Multiple influences of nitrate on uranium solubility during bioremediation of uranium-contaminated subsurface sediments. *Environ Microbiol* 4:510–516
- Gonzalez PJ, Correia C, Moura I, Brondino CD, Moura JGG (2006) Bacterial nitrate reductases: molecular and biological aspects of nitrate reduction. *J Inorg Biochem* 100:1015–1023
- Hansen HCB, Koch CB, Nancke-Krogh H, Borggaard OK, Sørensen J (1996) Abiotic nitrate reduction to ammonium: key role of green rust. *Environ Sci Technol* 30:2053–2056
- Hernandez ME, Newman DK (2001) Extracellular electron transfer. *Cell Mol Life Sci* 58:1562–1571
- Hoffmann MR, Martin ST, Choi W, Bahnemann BW (1995) Environmental applications of semiconductor photocatalysis. *Chem Rev* 95:69–96
- Holmes DE, Bond DR, Lovley DR (2004) Electron transfer by *Desulfobulbus propionicus* to Fe(III) and graphite electrodes. *Appl Environ Microbiol* 70:1234–1237
- Jørgensen CJ, Jacobsen OS, Elberling B, Aamand J (2009) Microbial oxidation of pyrite coupled to nitrate reduction in anoxic groundwater sediment. *Environ Sci Technol* 43:4851–4857
- Kanso SW, Greene AC, Patel BKC (2002) *Bacillus subtterraneus* sp. nov., an iron- and manganese-reducing bacterium from a deep subsurface Australian thermal aquifer. *Int J Syst Evol Microbiol* 52:869–874
- Kim BH, Kim HJ, Hyum MS, Park DH (1999) Direct electrode reaction of an Fe(III)-reducing bacterium, *Shewanella putrefaciens*. *J Microbiol Biotechnol* 9:127–131
- Li XM, Zhou SG, Li FB, Wu CY, Zhuang L, Xu W, Liu L (2009) Fe(III) oxide reduction and carbon tetrachloride dechlorination by a

- newly isolated *Klebsiella pneumoniae* strain L17. J Appl Microbiol 106:130–139
- Li FB, Li XM, Zhou SG, Zhuang L, Cao F, Huang DY, Xu W, Liu TX, Feng CH (2010) Enhanced reductive dechlorination of DDT in an anaerobic system of dissimilatory iron-reducing bacteria and iron oxide. Environ Pollut 158:1733–1740
- Li XM, Liu TX, Li FB, Zhang W, Zhou SG, Li YT (2011) Reduction of structural Fe(III) in oxyhydroxides by *Shewanella decolorationis* S12 and characterization of the surface properties of iron minerals. J Soils Sediments. doi:10.1007/s11368-011-0433-5
- Liu TX, Li XM, Li FB, Zhang W, Chen MJ, Zhou SG (2011) Reduction of iron oxides by *Klebsiella pneumoniae* L17: kinetics and surface properties. Colloid Surface A 379:143–150
- Lovley DR, Holmes DE, Nevin KP (2004) Dissimilatory Fe(III) and Mn(IV) reduction. Adv Microb Physiol 49:219–286
- Mimica D, Zagal JH, Bedioui F (2001) Electroreduction of nitrite by hemin, myoglobin and hemoglobin in surfactant films. J Electroanal Chem 497:106–113
- Moreno-Vivián C, Cabello P, Martínez-Luque M, Blasco R, Castillo F (1999) Prokaryotic nitrate reduction: Molecular properties and functional distinction among bacterial nitrate reductases. J Bacteriol 181:6573–6584
- Mori S, Ishii K, Hirakawa Y, Nakamura R, Hashimoto K (2011) In vivo participation of artificial porphyrins in electron-transport chains: electrochemical and spectroscopic analyses of microbial metabolism. Inorg Chem 50:2037–2039
- Nakamura R, Ishii K, Hashimoto K (2009a) In vivo participation of artificial porphyrins in electron-transport chains: electrochemical and spectroscopic analyses of microbial metabolism. Angew Chem Int Ed 48:1606–1608
- Nakamura R, Kai F, Okamoto A, Newton GJ, Hashimoto K (2009b) Self-constructed electrically conductive bacterial networks. Angew Chem Int Ed 44:508–511
- Nevin KP, Finneran KT, Lovley DR (2003) Microorganisms associated with uranium bioremediation in a high-salinity subsurface sediment. Appl Environ Microbiol 69:3672–3675
- Nimje VR, Chen CY, Chen CC, Jean JS, Reddy AS, Fan CW, Pan KY, Liu HT, Chen JL (2009) Stable and high energy generation by a strain of *Bacillus subtilis* in a microbial fuel cell. J Power Sources 190:258–263
- Obare SO, Ito T, Balfour MH, Meyer GJ (2003) Ferrous hemin oxidation by organic halides at nanocrystalline TiO<sub>2</sub> interfaces. Nano Lett 3:1151–1153
- Obuekwe CO, Westlake DWS (1982) Effect of reducible compounds (potential electron acceptors) on reduction of ferric iron by *Pseudomonas* species. Microbiol Lett 19:57–62
- Ottley CJ, Davison W, Edmunds WM (1997) Chemical catalysis of nitrate reduction by iron(II). Geochim Cosmochim Acta 61:1819–1828
- Paul T, Miller PL, Strathmann TJ (2007) Visible-light-mediated TiO<sub>2</sub> photocatalysis of fluoroquinolone antibacterial agents. Environ Sci Technol 41:4720–4727
- Pollock J, Weber KA, Lack J, Achenbach LA, Mormile MR, Coates JD (2007) Alkaline iron(III) reduction by a novel alkaliphilic, halotolerant *Bacillus* sp. isolated from salt flat sediments of Soap Lake. Appl Microbiol Biotechnol 77:927–934
- Rabaey K, Verstraete W (2005) Microbial fuel cells: novel biotechnology for energy generation. Trend Biotechnol 23:291–298
- Rajakumar S, Ayyasamy PM, Shanthi K, Thavamani P, Velmurugan P, Song YC, Lakshmanaperumalsamy P (2008) Nitrate removal efficiency of bacterial consortium (*Pseudomonas* sp. KW1 and *Bacillus* sp. YW4) in synthetic nitrate-rich water. J Hazard Mater 157:553–563
- Reguera G, McCarthy KD, Mehta T, Nicoll JS, Tuominen MT, Lovley DR (2005) Extracellular electron transfer via microbial nanowires. Nature 435:1098–1101
- Reiche M, Torburg G, Kusel K (2008) Competition of Fe(III) reduction and methanogenesis in an acidic fen. FEMS Microbiol Ecol 65:88–101
- Shen XY, Zhang LM, Shen JP, Li LH, Yuan CL, He JZ (2010) Soil type determines the abundance and community structure of ammonia-oxidizing bacteria and archaea in flooded paddy soils. J Soils Sediments 10:1510–1516
- Staniszewski A, Morris AJ, Ito T, Meyer GJ (2007) Conduction band mediated electron transfer across nanocrystalline TiO<sub>2</sub> surfaces. J Phys Chem B 111:6822–6828
- Straub KL, Benz M, Schink B, Widdel F (1996) Anaerobic, nitrate-dependent microbial oxidation of ferrous iron. Appl Environ Microbiol 62:1458–1460
- Stromberg JR, Wnuk JD, Pinlac RAF, Meyer GJ (2006) Multielectron transfer at heme-functionalized nanocrystalline TiO<sub>2</sub> reductive dechlorination of DDT and CCl<sub>4</sub> forms stable carbene compounds. Nano Lett 6:1284–1286
- Thauer RK, Jungermann K, Decker K (1977) Energy conservation in chemotrophic anaerobic bacteria. Bacteriol Rev 41:100–180
- Thygesen A, Poulsen FW, Min B, Angelidaki I, Thomsen AB (2009) The effect of different substrates and humic acid on power generation in microbial fuel cell operation. Biores Technol 100:1186–1191
- Wang XG, Liu CS, Li XM, Li FB, Zhou SG (2008) Photodegradation of 2-mercaptobenzothiazole in the  $\gamma$ -Fe<sub>2</sub>O<sub>3</sub>/oxalate suspension under UVA light irradiation. J Hazard Mater 153:426–433
- Wang XJ, Yang J, Chen XP, Sun GX, Zhu YG (2009) Phylogenetic diversity of dissimilatory ferric iron reducers in paddy soil of Hunan, South China. J Soils Sediments 9:568–577
- Weber KA, Picardal FW, Roden EE (2001) Microbially catalyzed nitrate-dependent oxidation of biogenic solid-phase Fe(II) compounds. Environ Sci Technol 35:1644–1650
- Weber KA, Urrutia MM, Churchill PF, Kukkadapu RK, Roden EE (2006) Anaerobic redox cycling of iron by freshwater sediment microorganisms. Environ Microbiol 8:100–113
- Xia X, Cao XX, Liang P, Huang X, Yang SP, Zhao GG (2010) Electricity generation from glucose by a *Klebsiella* sp. in microbial fuel cells. Appl Microbiol Biotechnol 87:383–390
- Xing SH, Chen CR, Zhou BQ, Zhang H, Nang YG, Xu ZH (2010) Soil soluble organic nitrogen and microbial processes under adjacent coniferous and broadleaf plantation forests. J Soils Sediments 10:748–757
- Xu Y, Schoonen MAA (2000) The absolute energy positions of conduction and valence bands of selected semiconducting minerals. Am Miner 85:543–556
- Yang L, Steefel CI, Marcus MA, Bargar JR (2010) Kinetics of Fe(II)-catalyzed transformation of 6-line ferrihydrite under anaerobic flow conditions. Environ Sci Technol 44:5469–5475
- Zhang SH, Cai LL, Liu Y, Shi Y, Li W (2009) Effects of NO<sub>2</sub><sup>-</sup> and NO<sub>3</sub><sup>-</sup> on the Fe(III)EDTA reduction in a chemical absorption–biological reduction integrated NOx removal system. Appl Microbiol Biotechnol 82:557–563
- Zhang YZ, Mo GQ, Li XW, Zhang WD, Zhang JQ, Ye JS, Huang XD, Yu CZ (2011) A graphene modified anode to improve the performance of microbial fuel cells. J Power Sources 196:5402–5407